J|A|C|S
ARTICLES
Published on Web 03/23/2007

Cluster Growth and Fragmentation in the Highly Fluxional Platinum Derivatives of Sn_9^{4-}: Synthesis, Characterization, and Solution Dynamics of $Pt_2@Sn_{17}^{4-}$ and $Pt@Sn_9H^{3-}$

Banu Kesanli, Jordan E. Halsig, Peter Zavalij, James C. Fettinger, Yiu-Fai Lam, and Bryan W. Eichhorn*

Contribution from the Department of Chemistry and Biochemistry, University of Maryland College Park, Maryland 20742

Received August 15, 2006; E-mail: eichhorn@umd.edu

Abstract: Sn_9^{4-} reacts with $Pt(PPh_3)_4$ in ethylenediamine/toluene solvent mixtures in the presence of 2,2,2-cryptand to give four different complexes: "Rudolph's complex" of proposed formula $[Sn_9Pt(PPh_3)_x]^{4-}$ (**2**), the previously reported $[Pt@Sn_9Pt(PPh_3)]^{2-}$ ion (**3**), and the title complexes $Pt_2@Sn_{17}^{4-}$ (**4**) and $Pt@Sn_9H^{3-}$ (**5**). The use of $Pt(norbornene)_3$ instead of $Pt(PPh_3)_4$ gives complex **4** exclusively. The structure of **4** contains two Pt atoms centered in a capsule-shaped Sn_{17} cage. The complex is highly dynamic in solution showing single, mutually coupled ^{119}Sn and ^{195}Pt NMR resonances indicative of an intramolecular liquidlike dynamic exchange process. Complex **5** has been characterized by selectively decoupled ^1H, ^{119}Sn, and ^{195}Pt NMR experiments and shows similar liquidlike fluxionality. In addition, the H atom scrambles across the cage showing small couplings to both Sn and Pt atoms. Neither **3** nor **4** obeys Wades rules; they adopt structures more akin to the subunits in alloys such as $PtSn_4$. The structural and chemical relevance to supported $PtSn_4$ heterogeneous catalysts is discussed.

Introduction

Platinum−tin intermetallics and composites are used in a variety of different heterogeneous catalytic applications that include catalytic reforming, low-temperature CO oxidation, and anodic methanol activation in fuel cells.[1−13] Although the systems have been studied extensively by many different groups, there are still many controversial issues regarding the active phases (e.g., discrete intermetallic particles of $PtSn_4$, PtSn, Pt_2Sn,...or phase separated aggregates), the oxidation states of the elements (Sn^0, Sn^{+2}, Sn^{+4}), and even the role of Sn in the catalytic process.[6,7,14,15] Even less is known about the mechanistic details on the molecular level. For example, the mechanism of hydrogen spillover, Pt migration, and substrate activation are critical features in catalyst function but are not well understood in these systems. However, it has been unequivocally shown that the bimetallic systems catalyze transformations that neither metal will promote individually. The remarkable low-temperature oxidation of CO and preferential oxidation of CO (PROX) using PtSn catalysts are excellent examples.[1,3,13]

Platinum−tin coordination compounds have been used both as molecular precursors for Pt−Sn heterogeneous bimetallic catalysts and to model the chemistry of the heterogeneous transformations in a homogeneous environment. While both methods have met with some success, the ancillary ligands (e.g., phosphines, halides) often interfere. For example, the use of organometallic precursors effectively produces PtSn bimetallic particles,[16−19] but they are often contaminated with chloride or other impurities.[16,17] The presence of Cl may actually enhance some catalytic transformations but complicates precursor strategies and mechanistic interpretation.

(1) Margitfalvi, J. L.; Borbath, I.; Hegedus, M.; Szegedi, A.; Lazar, K.; Gobolos, S.; Kristyan, S. *Catal. Today* **2002**, *73*, 343−353.
(2) Burch, R. *J. Catal.* **1981**, *71*, 348−359.
(3) Schuber, M. M.; Kahlich, M. J.; Feldmeyer, G.; Huttner, M.; Hackenberg, S.; Gasteiger, H. A.; Behm, R. J. *Phys. Chem. Chem. Phys.* **2001**, *3*, 1123−1131.
(4) Maroto, A.; Rodriguez-Ramos, I.; Guerrero-Ruiz, A.; Llorca, J.; de la Piscina, P. R.; Homs, N. *App. Organomet. Chem.* **2000**, *14*, 783−788.
(5) Margitfalvi, J. L.; Borbath, I.; Lazar, K.; Tfirst, E.; Szegedi, A.; Hegedus, M.; Gobolos, S. *J. Catal.* **2001**, *203*, 94−103.
(6) Davis, B. H. In *Platinum-Tin-Alumina Catalyst*; Davis, M. E., Suib, S. L., Eds.; ACS Symposium Series; American Chemical Society: Washington, DC, 1993; Vol. 517, p 109.
(7) Dupont, C.; Jugnet, Y.; Loffreda, D. *J. Am. Chem. Soc.* **2006**, *128*, 9129−9136.
(8) Okanishi, T.; Matsui, T.; Takeguchi, T.; Kikuchi, R.; Eguchi, K. *Appl. Catal. A* **2006**, *298*, 181−187.
(9) Lee, D.; Hwang, S.; Lee, I. *J. Power Sources* **2005**, *145*, 147−153.
(10) Radmilovic, V.; Richardson, T. J.; Chen, S. J.; Ross, P. N. *J. Catal.* **2005**, *232*, 199−209.
(11) Stamenkovic, V.; Grgur, B. N.; Ross, P. N.; Markovic, N. M. *J. Electrochem. Soc.* **2005**, *152*, A277−A282.
(12) Stamenkovic, V.; Arenz, M.; Blizanac, B. B.; Ross, P. N.; Markovic, N. M. *J. New Mater. Electrochem. Syst.* **2004**, *7*, 125−132.
(13) Schubert, M. M.; Kahlich, M. J.; Feldmeyer, G.; Huttner, M.; Hackenberg, S.; Gasteiger, H. A.; Behm, R. J. *Phys. Chem. Chem. Phys.* **2001**, *3*, 1123−1131.
(14) Margitfalvi, J. l.; Borbath, I.; Lazar, K.; Tfirst, E.; Szegedi, A.; Hegedus, M.; Gobolos, S. *J. Catal.* **2001**, *203*, 94−103.
(15) Burch, R.; Garla, L. C. *J. Catal.* **1981**, *71*, 360.
(16) Homs, N.; Llorca, J.; Ramirez, P.; Rodriguez-Reinoso, F.; Sepulveda-Escribano, A.; Silvestre-Albero, J. *Phys. Chem. Chem. Phys.* **2001**, *3*, 1782−1788.
(17) Carpenter, J. P.; Lukehart, C. M.; Stock, S. R. *J. Organomet. Chem.* **2000**, *596*, 252−256.
(18) Crabb, E. M.; Marshall, R.; Thompsett, D. *J. Electrochem. Soc.* **2000**, *147*, 4440−4447.
(19) Uchisawa, J. O.; Obuchi, A.; Zhao, Z.; Kushiyama, S. *Appl. Catal. B* **1998**, *18*, L183−L187.

An intriguing Pt−Sn model/precursor system involving the Sn_9^{4-} ion (**1**) and $Pt(PPh_3)_4$ was described by Rudolph et al. over 20 years ago.[20] Unlike the more common ligand stabilized PtSn complexes, the Rudolph system had the potential to provide ligand-free Pt−Sn complexes that could circumvent many of the complicating factors just described. In their studies, a Pt−Sn_9 complex was unequivocally identified by ^{119}Sn NMR spectroscopy,[20] but the structure and composition of the complex remain unknown. We subsequently showed[23] that addition of 2,2,2-crypt to the reaction generated the diplatinum $[Pt@Sn_9Pt(PPh_3)]^{2-}$ cluster along with Rudolph's original complex and other unidentified products. Herein we describe the remaining components of the reaction, $Pt_2@Sn_{17}^{4-}$ and $Pt@Sn_9H^{3-}$, and discuss their relationships to each other and the related clusters $Ni_2@Sn_{17}^{4-}$, $Pd_2@Ge_{18}^{4-}$, and $[Pt@Sn_9Pt(PPh_3)]^{2-}$.[21−23] The $Pt_2@Sn_{17}^{4-}$ cluster is a remarkable ligand-free PtSn binary complex, and $Pt@Sn_9H^{3-}$ shows a novel hydrogen scrambling process with potential relevance to hydrogen spillover processes in PtSn catalyzed processes.

Results

Synthesis. Ethylenediamine (en) solutions of K_4Sn_9 react with toluene solutions of $Pt(PPh_3)_4$ in the presence of 2,2,2-cryptand to give four different complexes. The products include Rudolph's complex of proposed formula "$[Sn_9Pt(PPh_3)_x]^{4-}$" (**2**), the previously reported[23] $[Pt@Sn_9Pt(PPh_3)]^{2-}$ ion (**3**), and the title complexes $Pt_2@Sn_{17}^{4-}$ (**4**) and $Pt@Sn_9H^{3-}$ (**5**). When the reaction is monitored by ^{119}Sn NMR spectroscopy, the resonances due to $[Pt@Sn_9Pt(PPh_3)]^{2-}$ and $Pt_2@Sn_{17}^{4-}$ ions are observed as soon as the reactants are mixed. The resonance for **2** is also present in the original mixture but increases in relative concentration over the first 24 h of reaction. The resonance for **5** only appears after ∼24 h of reaction.

Complexes **3** and **4** readily crystallize from solution as the $[(K(2,2,2\text{-crypt})]^+$ salts, whereas **2** and **5** have only been detected spectroscopically. Complex **3** crystallizes from solution in moderate yield (∼40%) after ∼24 h of reaction.[23] The crystals of $Pt_2@Sn_{17}^{4-}$ are obtained in lower yields (∼10%) from dilute solutions of the en/tol reaction mixture after the solution is completely depleted of **3** (ca. 1 week). When the reaction is conducted in the absence of 2,2,2-crypt, only Rudolph's complex **2** is observed in solution regardless of reaction time.

To avoid the competitive formation of **3**, complex **4** can be prepared as the exclusive product from the phosphine-free precursors Pt(norbornene)$_3$ and Pt(TMTVS), where TMVTS = 2,4,6,8-tetramethyl-2,4,6,8-tetravinylcyclotetrasiloxane. With the Pt(TMTVS) precursor under the same conditions, **4** appears within 24 h but slowly decomposes thereafter. The former precursor does not yield crystals of any product, whereas the Pt(norbornene)$_3$ precursor gives well formed crystals of **4** after 5 days in 13% yield.

The $[K(2,2,2\text{-crypt})]^+$ salt of $Pt_2@Sn_{17}^{4-}$ is very air and moisture sensitive in solution and the solid state. The salt is soluble in dmf and forms dark red-brown solutions. The complex has been characterized by single-crystal X-ray diffraction and ^{119}Sn and ^{195}Pt NMR spectroscopy. The $Pt@Sn_9H^{3-}$ ion (**5**) is formed as a trace component of the reactions described above and has not been isolated. The complex has been fully characterized by ^{1}H, ^{119}Sn, and ^{195}Pt NMR spectroscopy. The composition and the structure of the complex are based on NMR data and will be discussed in the next section.

We have previously shown[23] that the net oxidation of the reactants $Pt(PPh_3)_4$ and Sn_9^{4-} occurs by solvent reduction and subsequent H_2 evolution. The proposed *net* reactions for the formation of compounds **3**−**5** are given in eqs 1−3, respectively. However, the mechanisms of formation are likely to be quite complicated and involve interconversions of the various complexes. Because the composition and charge of Rudolph's complex, **2**, have not been established, the relationships between the various ions remain unknown.

$$Sn_9^{4-} + 2\,Pt(PPh_3)_4 + 2\,NH_2CH_2CH_2NH_2 \xrightarrow{(2,2,2\text{-crypt})} \underset{(\mathbf{3})}{[Pt@Sn_9Pt(PPh_3)]^{2-}} + 7PPh_3 + 2[H_2N(CH_2)_2NH]^{-1} + H_2 \quad (1)$$

$$2Sn_9^{4-} + 2\,Pt(PPh_3)_4 + 4NH_2CH_2CH_2NH_2 \xrightarrow{(2,2,2\text{-crypt})} \underset{(\mathbf{4})}{Pt_2@Sn_{17}^{4-}} + \text{“Sn”} + 4[H_2N(CH_2)_2NH]^{-1} + 8PPh_3 + 2H_2 \quad (2)$$

$$Sn_9^{4-} + Pt(PPh_3)_4 + NH_2CH_2CH_2NH_2 \xrightarrow{(2,2,2\text{-crypt})} \underset{(\mathbf{5})}{Pt@Sn_9H^{3-}} + [H_2N(CH_2)_2NH]^{-1} + 4PPh_3 \quad (3)$$

In the synthesis of **3**, N−H or C−H activation of the solvent (DMSO, en) to give H_2 gas was verified by H_2 trapping experiments.[23] The reduction of solvent molecules and ligands has also been documented in the formation of the $[E_7PtH(PPh_3)]^{2-}$ Zintl ions (E = P, As)[24,25] and other closely related complexes.[26,27] Since complexes **3**, **4**, and **5** form from the same reaction mixture, we assume that N−H activation is involved in the formation of all three complexes.

Solid-state Structure. The $[K(2,2,2\text{-crypt})]_4[Pt_2@Sn_{17}]$ salt crystallizes in two different polymorphs (I and II) that both suffer from disorder. Crystals of II are also badly twinned, but the Pt−Pt separations were clearly evident from a Patterson synthesis (∼4.2 Å) suggesting that the structures of the clusters are the same. In addition, both polymorphs have identical NMR spectroscopic signals. Only the details of I will be described here.

Polymorph I is triclinic, space group $P\bar{1}$, and contains four $[K(2,2,2\text{-crypt})]^+$ cations, one $Pt_2@Sn_{17}^{4-}$ anion, and three en solvate molecules in the crystal lattice. A summary of the crystallographic data is given in Table 1, and selected bond distances are listed in Table 2. Complete listings of bond

(20) Teixidor, F.; Leutkens, M. L., Jr.; Rudolph, R. W. *J. Am. Chem. Soc.* **1983**, *105*, 149−150.
(21) Esenturk, E. N.; Fettinger, J. C.; Eichhorn, B. W. *J. Am. Chem. Soc.* **2006**, *128*, 12−13.
(22) Goidoechea, J. M.; Sevov, S. C. *J. Am. Chem. Soc.* **2005**, *127*, 7676−7677.
(23) Kesanli, B.; Fettinger, J.; Gardner, D. R.; Eichhorn, B. *J. Am. Chem. Soc.* **2002**, *124*, 4779−4786.
(24) Kesanli, B.; Gardner, D. R.; Scott, B.; Eichhorn, B. W. *J. Chem. Soc., Dalton Trans.* **2000**, 1291−1296.
(25) Kesanli, B.; Charles, S.; Lam, Y.-F.; Fettinger, J. C.; Eichhorn, B. W. *J. Am. Chem. Soc.* **2000**, *122*, 11101−11107.
(26) Ugrinov, A.; Sevov, S. C. *Chem.—Eur. J.* **2004**, *10*, 3727−3733.
(27) Ugrinov, A.; Sevov, S. C. *J. Am. Chem. Soc.* **2003**, *125*, 14059−14064.

Table 1. Crystallographic Data for $[K(2,2,2\text{-crypt})]_3[Pt_2Sn_{17}]\cdot 3en$

empirical formula	$Pt_2Sn_{17}\cdot 4(C_{18}H_{36}N_2O_6)\cdot 3(C_2H_8N_2)$	
formula weight	4250.57	
temperature	220(2) K	
wavelength	0.71073 Å	
crystal system	triclinic	
space group	$P\bar{1}$	
unit cell dimensions	$a = 14.710(3)$ Å	$\alpha = 116.874(4)°$
	$b = 15.829(4)$ Å	$\beta = 96.699(4)°$
	$c = 16.253(4)$ Å	$\gamma = 100.299(4)°$
volume	3236.4(12) $Å^3$	
Z	1	
density, ρ_{calcd}	2.181 g/cm^3	
absorption coefficient, μ	5.553 mm^{-1}	
data/restraints/parameters	14639/670/911	
goodness-of-fit on F^2	1.052	
final R indices: R_1,[a] $I > 2\sigma(I)$	0.0372	
wR_2,[a] all data	0.0879	

[a] $R_1 = \Sigma||F_o| - |F_c||/\Sigma|F_o|$, $wR_2 = [\Sigma w(F_o^2 - F_c^2)^2/\Sigma w(F_o^2)^2]^{1/2}$, $w = 1/[\sigma^2(F_o^2) + (0.02P)^2 + 8.78P]$.

Table 2. Selected Bond Lengths (Å) for the $Pt_2@Sn_{17}^{4-}$ Ion

Pt−Sn1	2.780(1)	Pt−Sn2	2.814(2)	Pt−Sn3	2.745(1)
Pt−Sn4	2.815(2)	Pt−Sn5	2.803(2)	Pt−Sn6	2.804(2)
Pt−Sn7	2.672(1)	Pt−Sn8	2.770(2)	Pt−Sn9	2.804(2)
Sn7−Pt′	2.789(1)	Sn1−Sn4	3.032(2)	Sn1−Sn5	3.085(2)
Sn1−Sn6	3.093(1)	Sn1−Sn3	3.121(1)	Sn1−Sn2	3.305(2)
Sn2−Sn6	3.020(1)	Sn2−Sn3	3.107(2)	Sn2−Sn11	3.249(2)
Sn3−Sn7	3.022(2)	Sn3−Sn4	3.046(2)	Sn4−Sn5	2.980(2)
Sn4−Sn8	3.011(2)	Sn5−Sn6	3.120(2)	Sn5−Sn9	3.274(2)
Sn5−Sn8	3.371(2)	Sn6−Sn9	3.192(2)	Sn8−Sn9	3.017(2)
Sn9−Sn10	3.388(2)	Sn10−Sn11	2.958(2)	Sn7−Sn8	3.460(2)
Sn7−Sn11	3.405(2)				

distances and angles can be found in the Supporting Information. Several crystals of polymorph I were isolated from the various Pt precursors described in the previous section and were evaluated by single-crystal X-ray diffraction. In all cases, the $[K(2,2,2\text{-crypt})]^+$ cations were well-defined and not disordered. However, all determinations showed multiple orientations of the $Pt_2@Sn_{17}^{4-}$ anion that were also internally disordered. The $Pt(norbornene)_3$ precursor yielded the best quality crystals, which displayed one major orientation (76% occupancy) with two other minor contributors. The three orientations were successfully modeled and were shown to be identical. Only the major contributor is described here.

The $Pt_2@Sn_{17}^{4-}$ anion (Figure 1) has a capsulelike structure resulting from the oxidative coupling of two Pt-centered Sn_9^{4-} clusters with the formal extrusion of one Sn^{4-} ion. The anion is isoelectronic to the $Ni_2@Sn_{17}^{4-}$ anion (Figure 2c) but more structurally similar to $Pd_2@Ge_{18}^{4-}$ (Figure 2b).[22] The structure of $Pt_2@Sn_{17}^{4-}$ can be viewed as two $Pt@Sn_9$ subunits that share a common vertex, Sn7 (Figure 2a). The structure has two identical, $PtSn_6$ bicapped pentagonal prisms defined by planar Sn_5 rings (Sn2−Sn3−Sn4−Sn5−Sn6) capped by Sn1 and Pt. The $PtSn_6$ subunits are fused by the central, planar five-membered ring defined by Sn7−Sn8−Sn9−Sn10−Sn11. The $Pd_2@Ge_{18}^{4-}$ ion has virtually identical $PdGe_6$ subunits, but they are fused by a central, planar Ge_6 ring (Figure 2b).[22] In $Pt_2@Sn_{17}^{4-}$, the central five-membered ring is flat but highly distorted (see below and Figure S-1) leaving only a virtual C_2 axis defined by Sn7 and the midpoint of the Sn9−Sn10 bond. Although the $Pt_2@Sn_{17}^{4-}$ ion has only C_2 molecular point symmetry, the ion resides on a crystallographic inversion center where the point of inversion is in the center of the Sn_7-Sn_{11} ring. This symmetry operation generates an identical orientation of the central ring that is rotated by 36° from the original. Each orientation is 50% occupied in the crystal lattice (Figure S-2), but only one orientation is shown in Figure 1. This disorder only affects the central ring and is equivalent to flipping the cluster upside down, which interchanges the top and bottom fragments. The crystallographic positions of the top and bottom

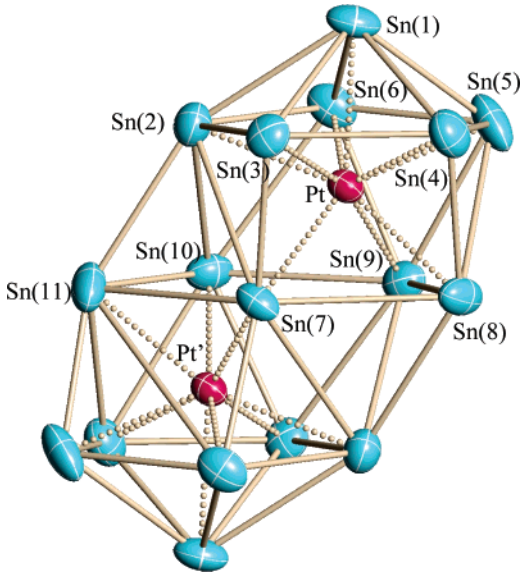

Figure 1. X-ray structure of the $Pt_2@Sn_{17}^{2-}$ ion. Thermal ellipsoids drawn at the 50% probability level.

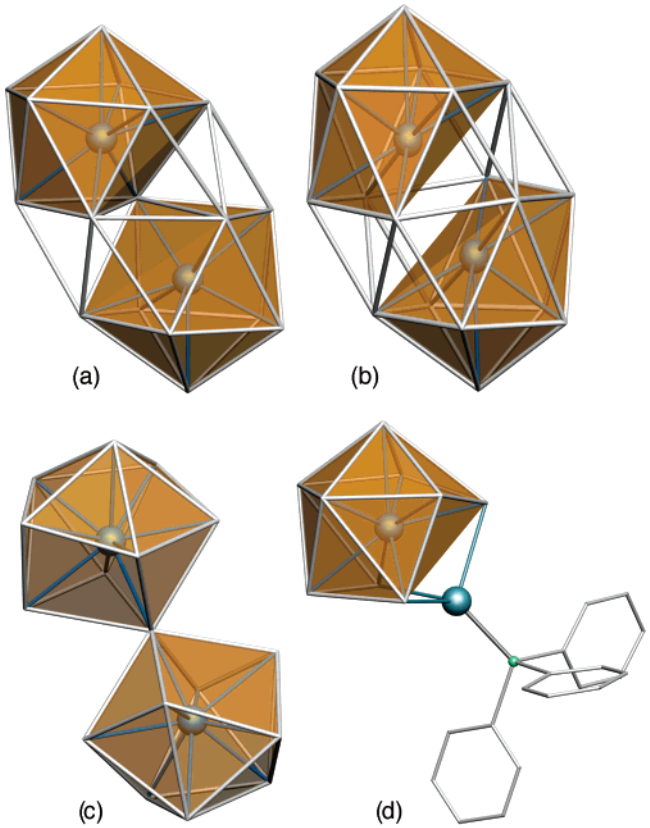

Figure 2. Polyhedral representation of (a) $Pt_2@Sn_{17}^{4-}$, (b) $Pd_2@Ge_{18}^{4-}$ from ref 22, (c) $Ni_2@Sn_{17}^{4-}$ from ref 21, and (d) $Pt@Sn_9Pt(PPh_3)^{2-}$ from ref 23. The translucent nine-vertex orange polyhedra show the transition metal coordination spheres in the respective clusters. The silver bars represent Sn−Sn or Ge−Ge bonds.

$PtSn_6$ segments are the same in both orientations. As such, superposition of the two orientations generates a crystallographic inversion center and a disorder in the central ring.

The $Pt_2@Sn_{17}^{4-}$, $Pd_2@Ge_{18}^{4-}$, and $Ni_2@Sn_{17}^{4-}$ structures (Figure 2a−c) have very similar metal-centered $M@E_9$ subunits (M═Ni, Pd, Pt; E = Ge, Sn) that are derived from well-known D_{3d} tricapped trigonal prismatic $E_9^{4-/3-/2-}$ clusters.[28−34] Similar structural units can now be found in many centered Zintl ions, such as the $[Pt@Sn_9Pt(PPh_3)]^{2-}$ (Figure 2d),[23] $[Ni@Ge_9Ni(PPh_3)]^{2-}$, and $Ni_3@Ge_{18}^{4-}$ complexes.[23,35,36] In all of the metal-centered clusters, the central E_9 units are distorted to various degrees, but all examples have very similar symmetrical ME_6 subunits defined by planar E_5 rings (E = Sn, Ge) capped by the centered transition metal on one side and a μ_5-E atom on the other. In the present structure, the top and bottom rings have Sn−Sn−Sn angles of 107.9° ± 1.7° with all the angles in the range 105.3°−109.4°. In contrast, the central ring is flat but highly distorted. The Sn−Sn−Sn angles average 107.9° ± 26.8° but vary from 77.7° to 138.8°. The obtuse Sn11−Sn7−Sn8 angle of 138.8(12)° allows Sn7 to form bonds to both Pt and Pt′ but leads to a large distortion in the cluster.

The Pt atoms make relatively uniform bonds to nine tin atoms; including three bonds each to the central Sn_5 ring. The Pt−Sn distances average 2.78(5) Å (av) with all 18 contacts within the range 2.672(1)−2.815(2) Å. For comparison, the $Pt_{centered}$−Sn bond distances in the related $[Pt@Sn_9Pt(PPh_3)]^{2-}$ ion are in the range 2.675(3)−2.793(2) Å, respectively. The Pt−Pt distance in the $Pt_2@Sn_{17}^{4-}$ complex (4.194(2) Å) is a nonbonding separation. The shortest Pt−Sn contact (2.672(1) Å) is to Sn7, which is the only Sn atom bonded to both Pt atoms. Interestingly, the shortest Ni−Sn contact in $Ni_2@Sn_{17}^{4-}$ is also to the bridging Sn7 atom (Figure 2c). The Sn−Sn contacts are in the range 3.03(2)−3.46(2) Å.

The $Pt_2@Sn_{17}^{4-}$ complex has 38 electrons according to Wade's rules[37,38] where the Sn atoms contribute 34 electrons to the cluster bonding (2 e^- each), the charge provides 4 e^-, and the centered Pt atoms contribute zero. However, the 17-vertex system is larger than those typically classified under these bonding schemes, and Wades rules do not seem amenable to multifocus clusters.[36,39] The structure of $Pt_2@Sn_{17}^{4-}$ does not fit into a classical deltaheldral bonding model and joins the growing class of multifocus deltahedral-like Zintl clusters with nontraditional structures, such as $Ni_2@NiGe_{18}^{4-}$, $Pd_2@Ge_{18}^{4-}$, and $[Ni_2@Ge_{13}Ni_4(CO)_5]^{4-}$.[35,36,39]

In the case of the $Pt@Sn_9H^{3-}$ complex, there are 22 electrons and 9 vertices in the cluster, which is similar to the case for the parent *nido*-Sn_9^{4-} ion. However, the structure is also not likely to be a classical Wadian cluster (see next section).

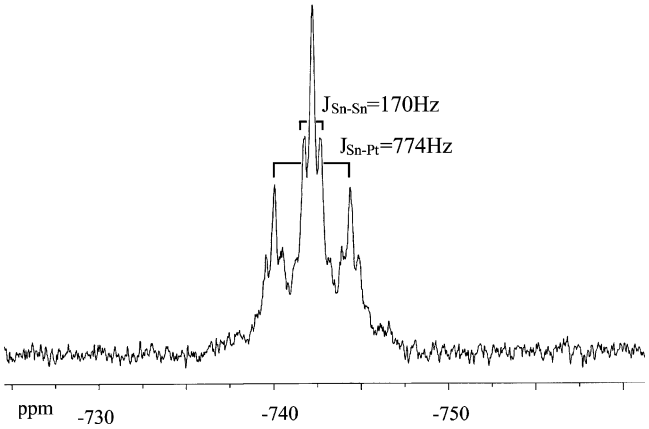

Figure 3. ^{119}Sn NMR spectrum of $Pt_2@Sn_{17}^{4-}$ recorded from dmf solutions at 25 °C.

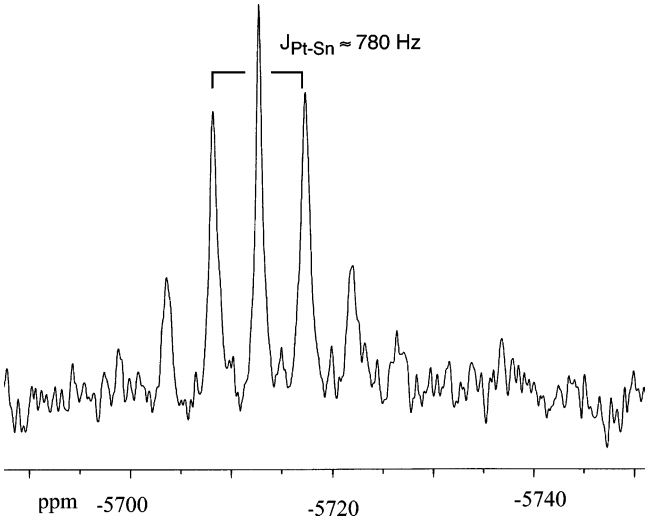

Figure 4. ^{195}Pt NMR spectrum of $Pt_2@Sn_{17}^{4-}$ recorded from dmf solutions at 25 °C.

NMR Spectroscopic Studies. 1. $Pt_2@Sn_{17}^{4-}$: The ^{195}Pt and ^{119}Sn NMR data are consistent with the nuclearity of the $Pt_2@Sn_{17}^{4-}$ complex but not with the solid-state structure. The room temperature ^{119}Sn spectrum (^{119}Sn, $I = {}^1/_2$, 8.7% abund.) shows a single ^{119}Sn resonance at −742.3 ppm flanked by one set of ^{195}Pt satellites (^{195}Pt, $I = {}^1/_2$, 33.7% abund.) with $^1J_{^{195}Pt-^{119}Sn} = 774$ Hz due to the coupling to the interstitial Pt atoms (Figure 3). For comparison, this coupling constant is less than half of the 1690 Hz $^{195}Pt-^{119}Sn$ coupling to the centered Pt in $[Pt@Sn_9Pt(PPh_3)]^{2-}$. Moreover, the intensities of the ^{195}-Pt satellites indicate equal coupling to the two equivalent Pt atoms of the $Pt_2@Sn_{17}^{4-}$ cluster. The ^{119}Sn resonance also has ^{117}Sn satellites (^{117}Sn, $I = {}^1/_2$, 7.7% abund.) with $^1J_{^{117}Sn-^{119}Sn} =$ 170 Hz and intensities consistent with a 17-atom tin cluster. The ^{195}Pt NMR spectrum (Figure 4) also shows a single resonance, centered at −5713 ppm, with a satellite pattern due to coupling to all 17 tin atoms. The coupling constant ($^1J_{^{195}Pt-^{119/117}Sn} \approx 780$ Hz) equals that observed in the ^{119}Sn NMR spectrum.

All 17 Sn atoms of the $Pt_2@Sn_{17}^{4-}$ complex are time averaged in solution and couple equally to the two centered Pt atoms. The exchange process is intramolecular (no loss of coupling) and remains rapid on the NMR timescale at −60 °C. These data are consistent with a liquidlike scrambling of the Sn atoms around the Pt atoms. The dynamic process is similar to that

(28) Yong, L.; Hoffmann, S. D.; Fassler, T. F. *Z. Anorg. Allg. Chem.* **2005**, *631*, 1149−1153.
(29) Fassler, T. F.; Hoffmann, S. D. *Angew. Chem., Int. Ed.* **2004**, *43*, 6242−6247.
(30) Grützmacher, H.; Fassler, T. F. *Chem.—Eur. J.* **2000**, *6*, 2317−2325.
(31) Corbett, J. D. *Chem. Rev.* **1985**, *85*, 383−397.
(32) Goicoechea, J. M.; Sevov, S. C. *Inorg. Chem.* **2005**, *44*, 2654−2658.
(33) Goicoechea, J. M.; Sevov, S. C. *J. Am. Chem. Soc.* **2004**, *126*, 6860−6861.
(34) Guloy, A. M. *J. Am. Chem. Soc.* **1998**, *120*, 7663.
(35) (a) Esenturk, E. N.; Fettinger, J.; Eichhorn, B. *Polyhedron* 2006, *25*, 521−529. (b) Goicoechea, J. M.; Sevov, S. C. *J. Am. Chem. Soc.* **2006**, *128*, 4155−4161.
(36) Goicoechea, J. M.; Sevov, S. C. *Angew. Chem., Int. Ed.* **2005**, *44*, 4026−4028.
(37) Wade, K. J. *Adv. Inorg. Chem. Radiochem.* **1976**, *18*, 1.
(38) Wade, K. *Chem. Britain* **1975**, *11*, 177−183.
(39) Ugrinov, A.; Sevov, S. C. *Comp. Rend. Chim.* **2005**, *8*, 1878−1882.

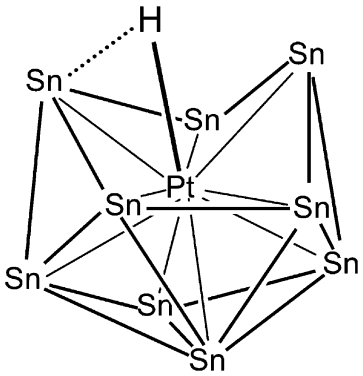

Figure 5. Proposed structure of $Pt@Sn_9H^{3-}$ ion.

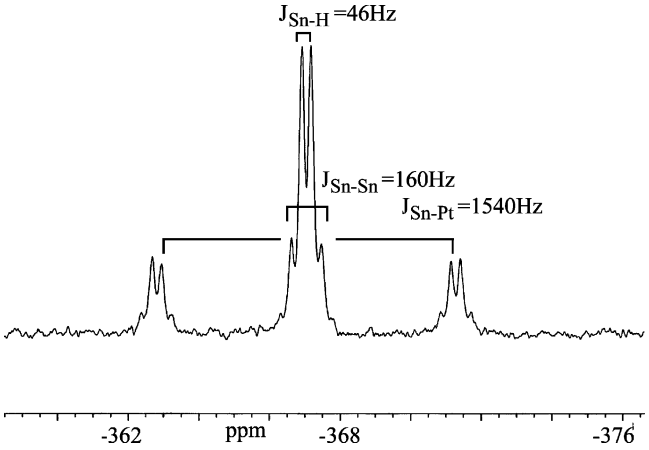

Figure 6. ^{119}Sn NMR spectrum of $Pt@Sn_9H^{3-}$ recorded from en/tol solutions at 25 °C.

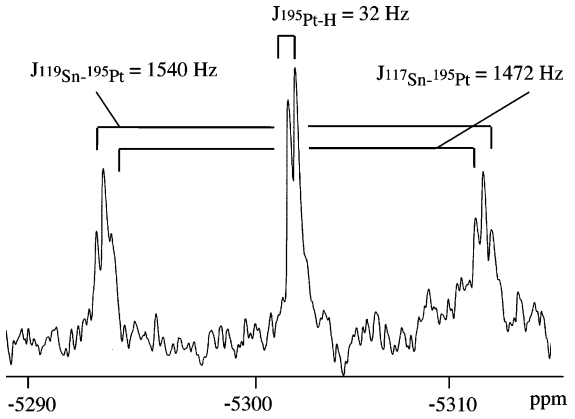

Figure 7. ^{195}Pt NMR spectrum of the $Pt@Sn_9H^{3-}$ ion recorded from en/tol solutions at 25 °C.

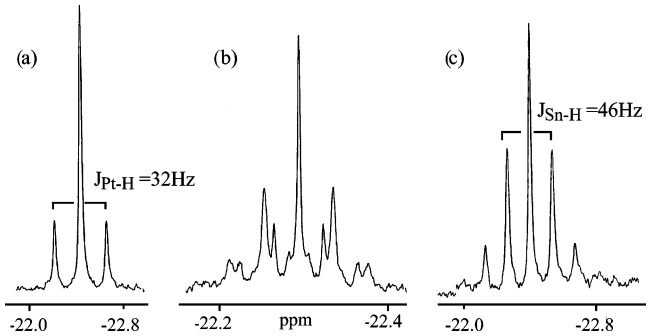

Figure 8. (a) $^{119/117}$Sn decoupled ^{1}H NMR, (b) ^{1}H NMR (coupled to $^{119/117}$Sn and ^{195}Pt), and (c) ^{195}Pt decoupled ^{1}H NMR spectra of $Pt@Sn_9H^{3-}$ ion recorded from en/tol-d_8 solutions at 25 °C.

observed for $Ni_2@Sn_{17}^{4-}$ and $[Pt@Sn_9Pt(PPh_3)]^{2-}$ and is discussed further in the discussion section.

2. $Pt@Sn_9H^{3-}$ (5): The structure and the composition of this complex are based on the ^{1}H, ^{119}Sn, and ^{195}Pt NMR spectra. The proposed structure comprises a nine-atom tin cluster with an interstitial Pt atom and a hydrogen atom (see Figure 5). The structure of the $Pt@Sn_9H^{3-}$ complex (**5**) can be viewed as a fragment of the $Pt_2@Sn_{17}^{4-}$ complex with an additional hydride ligand. Although the number of Sn atoms cannot be unequivocally proven by the NMR data alone, the NMR data and structural precedence in the literature[20,25,40−42] give strong support for the proposed structure as discussed below.

The ^{119}Sn spectrum of **5** (Figure 6) shows a single resonance at −368 ppm that is split into a doublet due to coupling to the hydride ($J^{119}_{Sn-^1H}$ = 46 Hz). The peak also has a single set of ^{195}Pt satellites ($J^{195}_{Pt-119Sn}$ = 1540 Hz, 33% intensity) and ^{117}Sn satellites ($J^{119}_{Sn-117Sn}$ = 160 Hz). Similarly, the ^{195}Pt NMR spectrum shows resonance centered at −5303 ppm (see Figure 7) that is also split into a doublet due to coupling to the hydride ($J^{195}_{Pt-^1H}$ = 32 Hz). Two sets of tin satellites can be resolved ($^1J^{195}_{Pt-119Sn}$ = 1540 Hz; $^1J^{195}_{Pt-117Sn}$ = 1472 Hz) with integrated intensities consistent with nine equivalent Sn atoms.

The doublet structure of the ^{119}Sn and ^{195}Pt resonances arises from the presence of a single hydrogen atom. Because of the difficulty in locating the lone, low intensity ^{1}H NMR signal associated with a trace amount of **5** amidst the intense solvent and cation peaks, it was necessary to search for the ^{1}H NMR resonance by decoupling 1000 Hz blocks of the ^{1}H spectrum while observing the ^{119}Sn NMR signal (manual inverse detection). The ^{1}H NMR signal for the hydride was located at −22.3 ppm and displayed a second-order set of $^{119/117}$Sn and ^{195}Pt satellites (Figure 8b). The satellites are readily assigned through selective decoupling experiments and comparisons to the coupling constants observed in the ^{119}Sn and ^{195}Pt NMR spectra ($J^{195}_{Pt-^1H}$ = 32 Hz; $J^{119}_{Sn-^1H}$ = 46 Hz). Decoupling of both tin isotopomers (^{119}Sn and ^{117}Sn) at the same time results in a ^{1}H NMR signal with only ^{195}Pt satellites (Figure 8a). The intensity of the satellites signifies coupling to only one Pt center. Similarly, the ^{195}Pt decoupled ^{1}H NMR spectrum shows only $^{119/117}$Sn satellites consistent with the presence of nine tin atoms (Figure 8c).

The nuclearity of the Sn cluster is readily determined from the satellite intensities on ^{1}H and ^{195}Pt resonances and comparisons with the spectra of the $[Pt@Sn_9Pt(PPh_3)]^{2-}$ and $Pt_2@Sn_{17}^{4-}$ complexes. The assessment is as follows: (1) The presence of a single peak in ^{195}Pt NMR and the ^{195}Pt satellite intensities on ^{1}H and ^{119}Sn resonances show that there is only one Pt atom in the complex. (2) Both ^{119}Sn and ^{195}Pt resonances are split into doublets, indicating the presence of a single hydrogen atom. (3) The $^{119/117}$Sn satellite intensities on the ^{1}H and ^{195}Pt resonances as well as the ^{117}Sn satellite intensities on the ^{119}Sn resonance are consistent with a nine-atom tin cluster and are very similar to those of $[Pt@Sn_9Pt(PPh_3)]^{2-}$. Different nuclearity clusters, such as HSn_8Pt and $HSn_{10}Pt$, cannot be ruled

(40) Eichhorn, B. W.; Haushalter, R. C.; Pennington, W. T. *J. Am. Chem. Soc.* **1988**, *110*, 8704−8706.
(41) Kesanli, B.; Fettinger, J. C.; Gardner, D. R.; Eichhorn, B. W. *Chem.—Eur. J.* **2001**, 5277−5285.
(42) Campbell, J.; Mercier, H. P. A.; Holger, F.; Santry, D.; Dixon, D. A.; Schrobilgen, G. J. *Inorg. Chem.* **2002**, *41*, 86−107.

out by satellite intensity alone; however, due to the ubiquitous formation of Sn_9 complexes from polystannide solutions and the collective NMR properties (chemical shifts, coupling constants, *and* satellite intensities), the formula of the complex is assigned as $Pt@Sn_9H$.

Because the $Pt@Sn_9H$ complex is diamagnetic, electron counting protocols indicate either 20 electrons ($2n + 2$) or 22 electrons ($2n + 4$) for a nine-vertex cluster, suggesting charges of $Pt@Sn_9H^{1-}$ or $Pt@Sn_9H^{3-}$, respectively. Although either scenario is possible, we favor the -3 charge due to its solubility and stability. Soluble Zintl ions or metalated Zintl ion complexes with a -1 charge have not been reported to date, whereas -2, -3, and -4 charges are common.

Although the nuclearity of the $Pt@Sn_9H^{3-}$ ion is evident from the NMR data, deduction of the structure from this data is complicated by the fluxional nature of the complex (see below). Based on previous spectroscopic and structural studies of related Sn_9M systems, there are two viable structure types for **5**. The cluster could adopt a 10-vertex type structure with the Pt atom in a capping position (cf. the $[Sn_9M(CO)_3]^{4-}$ complexes).[40−42] Alternatively, the Pt atom could occupy an interstitial position as in the case of $[Pt@Sn_9Pt(PPh_3)]^{2-}$ and $Pt_2@Sn_{17}^{4-}$. The NMR data strongly support the latter with the Pt atom in an interstitial site. Comparisons with the NMR data of $[Pt@Sn_9Pt(PPh_3)]^{2-}$, **3**, which has both capping and interstitial Pt atoms, illustrate the point. The $^{195}Pt-^{119}Sn$ coupling constant of 1540 Hz in **5** is very close to the 1690 Hz interstitial $^{195}Pt-^{119}Sn$ coupling observed in $[Pt@Sn_9Pt(PPh_3)]^{2-}$. By contrast, the $^{195}Pt-^{119}Sn$ coupling constant to the capping Pt in **3** is less than 50 Hz as a result of averaging associated with exchange processes. Moreover, the $^{119/117}Sn$ satellite pattern on the ^{195}Pt resonance of **5** is quite similar to that of the interstitial Pt atom and differs from that of the capping Pt atom in the $[Pt@Sn_9Pt(PPh_3)]^{2-}$ complex. In total, the data are consistent with a structure containing an interstitial Pt encapsulated by the nine tin atoms. The proposed structure shown in Figure 5 is essentially replacement of the $Pt(PPh_3)$ fragment of $[Pt@Sn_9Pt(PPh_3)]^{2-}$ with H^- and is fully consistent with the NMR data.

The $Pt@Sn_9H^{3-}$ complex shows dynamic behavior similar to that of $[Pt@Sn_9Pt(PPh_3)]^{2-}$ and $Pt_2@Sn_{17}^{4-}$. All nine Sn atoms are equivalent on the NMR timescale giving rise to a single peak in the ^{119}Sn NMR spectrum. The large $^{195}Pt-^{119}Sn$ coupling shows that the Pt atom remains bound to the Sn_9 cluster during the fluxional process.

The most unusual feature of **5** involves the fluxionality of the hydride ligand. The high field ^1H NMR chemical shift is suggestive of a Pt−H complex, but the coupling constant is much smaller than those of typical Pt−H species. For example, the Pt−H coupling constant in the $[P_7PtH(PPh_3)]^{2-}$ complex ($^1J_{Pt-H}$ is 1080 Hz)[43] is significantly larger than the 32 Hz observed in **5**. The observed 46 Hz $^{119}Sn-^1H$ coupling constant in **5** is also much less than the typical values, such as in the case of Bu_2SnIH where $^1J_{^{119}Sn-^1H} = 2060$ Hz.[44] The small coupling constants suggest that the H atom is either semi-bridging between the Pt and the scrambling Sn_9 cage or is rapidly scrambling around the outside surface of the cluster between the Pt and Sn atoms. Both processes will generate time-averaged values significantly less than expected static, single-bond couplings. Although the scrambling is fast on the NMR time scale, the process must be intramolecular as coupling is maintained in the fast exchange limit. It is interesting to note that the hydride ligands in the closely related $[E_7PtH(PPh_3)]^{2-}$ ions (E = P, As)[43] apparently do not scramble across the cluster surfaces nor do they form semi-bridging sites. However, the site of hydrogen attachment can vary between the main group cage and the transition metal on closely related clusters (e.g., $[P_7PtH(PPh_3)]^{2-}$ with Pt−H and $[P_7NiH(PPh_3)]^{2-}$ with a P−H).[43]

The fluxionality of the parent Sn_9^{4-} Zintl ion is well established, and the only static complexes isolated to date are $[(\eta\text{-}C_7H_8)Nb(\textit{cyclo}\text{-}Sn_6)Nb(\eta\text{-}C_7H_8)]^{2-}$ and $[Sn_6\{Cr(CO)_5\}_6]^{2-}$.[45,46] All *closo*-$[Sn_9M(CO)_3]^{4-}$ (M = Cr, Mo, W) complexes show local fluxionality at best.[41,42] The $Pt@Sn_{17}^{4-}$ cluster is fluxional in such a way that all of the 17 tin atoms are in fast exchange and give rise to a single ^{119}Sn resonance. The exchange of all 17 Sn atoms across the 2 Pt centers explains why the $J^{195}_{Pt-^{119}Sn} = 774$ Hz observed in $Pt_2@Sn_{17}^{4-}$ is approximately half of that in $[Pt@Sn_9Pt(PPh_3)]^{2-}$ ($J^{195}_{Pt-^{119}Sn} = 1690$ Hz) and $Pt@Sn_9H^{3-}$ ($J^{195}_{Pt-^{119}Sn} = 1540$ Hz). In the latter clusters, the nine Sn atoms in exchange maintain bonding to the centered Pt atom and direct Pt−Sn bonding is never compromised. In contrast, each Sn atom in $Pt_2@Sn_{17}^{4-}$ is bonded to a specific Pt atom only 50% of the time, which reduces its coupling constant relative to the single focus clusters.

The site exchange in the $Pt_2@Sn_{17}^{4-}$ ion is apparently faster than that in the isoelectronic $Ni_2@Sn_{17}^{4-}$ cluster. As such, the limiting ^{119}Sn spectrum can be obtained for $Ni_2@Sn_{17}^{4-}$ but not for $Pt_2@Sn_{17}^{4-}$ under identical conditions. The $Pt_2@Sn_{17}^{4-}$ structure is most likely a transition state in the $Ni_2@Sn_{17}^{4-}$ exchange process. The structures are closely related as shown in Figure 2. By breaking the seven Sn−Sn bonds between the $Pt@Sn_9$ subunits (i.e., those bonds that are not part of the orange polyhedra in Figure 2a), one obtains the $Ni_2@Sn_{17}^{4-}$ structure shown in Figure 2c. Since we know intramolecular bond breaking and bond making are facile under these conditions and recognize the similarities in the bridging M−Sn(7)−M units, it seems likely that the structures represent two local minima on the dynamic exchange pathway.

Discussion

The reaction between $Pt(PPh_3)_4$ and Sn_9^{4-} produces four different compounds as a function of time and reaction conditions. The synthesis and study of the title anions are important for several reasons. (1) They are examples of the growing class of ligand-free and "lightly ligated" group 14 transition metal clusters. These charged molecular intermetallics have unique structures and dynamic properties that distinguish them from other Zintl complexes and related organometallic model cluster systems. (2) Their structures and dynamic properties provide insight into the atomistic processes occurring on supported PtSn catalysts. (3) The stoichiometric activation of saturated solvent molecules during the synthesis of **2**−**5** illustrates their remarkable nucleophilicity. (4) These complexes serve as room-temperature single-source precursors to PtSn alloys. Items 1−3

(43) Charles, S.; Eichhorn, B. W.; Bott, S. G.; Fettinger, J. C. *J. Am. Chem. Soc.* **1996**, *118*, 4713−4714.
(44) Sawyer, A. K.; Brown, Y. E.; Hanson, E. L. *J. Organomet. Chem.* **1965**, *3*, 464−468.
(45) Kesanli, B.; Eichhorn, B. W.; Fettinger, J. C. *Angew. Chem., Int. Ed.* **2001**, *40*, 2300−2302.
(46) Schiemenz, B.; Huttner, G. *Angew. Chem., Int. Ed.* **1993**, *32*, 297−298.

are discussed individually below. Item 4 will be described in a subsequent publication.

Of the two complexes that have been structurally characterized (**3** and **4**), neither follows traditional molecular bonding schemes (i.e., Wades rules) or possesses familiar cluster-type structures. The cluster geometries more closely resemble the structural subunits in the known PtSn binary alloys. Jeitschko et al.[47] reported the structures of various M−Sn binary alloys such as $PtSn_4$, thus providing accurate descriptions of the Sn and Pt coordination environments and interatomic distances. In the $PtSn_4$ alloy, each Pt atom is in a tetragonal antiprism of Sn atoms, which is very similar to the coordination polyhedra of Pt and Sn atoms in $Pt_2@Sn_{17}^{4-}$ and the related $[Ni@Sn_9Ni(CO)]^{3-}$ ion.[23] The Pt−Sn and Sn−Sn distances observed for $[Pt@Sn_9Pt(PPh_3)]^{2-}$ and $Pt_2@Sn_{17}^{4-}$ are also quite similar to those in $PtSn_4$ as well. Not surprisingly, the oxidation of the clusters leads to room temperature formation of $PtSn_4$, which will be described in a subsequent publication.

The formation and dynamic behavior of complexes **4** and **5**, including the coupling of the $PtSn_9$ units to form larger PtSn clusters (i.e., $Pt_2@Sn_{17}^{4-}$), may be viewed as a model for particle growth and the well-known Pt migratory aging process in the bimetallic PtSn catalyst systems.[48] During catalysis, the Pt atoms in PtSn alloys migrate from active surface sites to inactive bulk sites that are encapsulated in Sn matrices. This process depletes the catalyst surface of active Pt atoms and leads to activity loss with aging. The recurring liquidlike behavior and the preference of Pt for interstitial sites in clusters **2**−**5** suggests that Pt mobility is quite facile in small particles and is consistent with the aging problems occurring in the supported systems.

The intramolecular scrambling of the hydrogen atom in $Pt@Sn_9H^{3-}$ was unexpected in light of the static nature of the hydrides in related complexes (e.g., $[P_7PtH(PPh_3)]^{2-}$).[44] This unusual scrambling contradicts the current models in PtSn catalytic systems where hydrogen spillover is proposed to be a Pt-mediated event.[3,49] The facile H scrambling could explain some of the anomalous features associated with excess H atom spillover in PtSn systems. The scrambling of H in the $Pt@Sn_9H^{3-}$ complex suggests that H atoms could migrate between Pt and Sn on a PtSn surface.

The C−H and N−H activations of the solvent with the evolution of H_2 gas in the synthesis of **3**−**5** is quite similar to the catalytic reforming processes occurring on PtSn catalysts. However, the activation of solvent in these reactions is stoichiometric and not catalytic. It is important to note that activation of solvent does not occur before the addition of 2,2,2-crypt to the reaction mixture, which suggests that Rudolph's original complex **2** is not oxidized or protonated. Presumably, the ion pairing between the alkali ions in solution and Rudolph's complex reduces the nucleophilicity of the Pt atom enough to preclude solvent activation.

Finally, the $Pt_2@Sn_{17}^{4-}$ ion is a member of the new ligand-free "intermetalloid" cluster family[21,22,29,36,50,52] defined by large bimetallic clusters with structures in between those of molecules and intermetallic solids. These clusters bridge the gap between bimetallic molecular clusters and bimetallic nanoparticles with bulk solid-state structures.

In summary, we have identified and characterized three of the four products formed in the reaction between $Pt(PPh_3)_4$ and Sn_9^{4-} and studied their structures and solution dynamics. The three complexes, $[Pt@Sn_9Pt(PPh_3)]^{2-}$, $Pt_2@Sn_{17}^{4-}$, and $Pt@Sn_9H^{3-}$, adopt structures that differ from those of the classical Zintl ion complexes and do not necessarily follow Wades rules of electron counting. All of the complexes are highly dynamic in solution such that the tin clusters show liquidlike behavior with intramolecular exchange of all sites. The hydrogen in $Pt@Sn_9H^{3-}$ scrambles between both the Pt and Sn sites in an unexpected multisite exchange. The structures and dynamic properties of these ions provide insight into the chemistry occurring on heterogeneous PtSn supported catalysts.

Experimental Section

General Data. All reactions were performed in a nitrogen filled drybox (Vacuum Atmospheres Company). ^{1}H (500 MHz) NMR spectra were recorded with a Bruker AVANCE DRX500 spectrometer, with four RF transmitters and amplifiers. Selective proton/tin decoupling experiments were conducted with a custom-made 5 mm triple-inverse probe with a Z-gradient (Bruker PZ 5722/001) in which the ^{1}H is the inner observe coil. One of the outer coils is fixed for Sn-117, and the other outer coil is a broad band (tunable to ^{119}Sn or ^{195}Pt) depending on the desirable decoupling nucleus. Custom-made H2 stop filters were used in both decoupling transmitter inputs to the probe. The pulse sequence used was modified from the standard Bruker "zgdc" by adding a third nucleus for simultaneous decoupling. GARP sequences were used in both decoupling nuclei in all cases. The digital FID resolution was 0.25 Hz/point for all inverse ^{1}H detections. Routine direct observe ^{119}Sn (149 MHz) and ^{195}Pt (85.9 MHz) NMR measurements were carried out with a Bruker Model AVANCE AV-400 NMR spectrometer, on a 5 mm broad-band probe. ^{1}H (400 MHz) decoupling was used as needed. In all measurements, to avoid RF heating, a high nitrogen flow rate was used in combination with the temperature controller. Sufficient prerequisition scans (typically 128 dummy scans) were activated to ensure the stability of the lock and field homogeneity. The pulse sequence used was the standard Bruker "zgdc" program. A 30° pulse strength and relaxation delays (1.0 s for ^{195}Pt and 0.5 s for all the others) were used. A macro automation program was written so that multiple block searches of 500 ppm and 800 ppm spectral widths were used in locating the ^{119}Sn and ^{195}Pt signals, respectively. Typically, each block acquisition time was 1 to 2 h, and the multiple block searches required up to 24 h of instrument time. The signals were confirmed and verified by repeating the final measurements with different transmitter offsets. ^{119}Sn chemical shifts were referenced to Me_4Sn in C_6D_6 (0 ppm). An aqueous solution of $[PtCl_6]^{2-}$ (0 ppm) was used for the ^{195}Pt NMR experiments. dmf-d_7/tol-d_8 mixtures were used as an internal reference for low-temperature studies. Block searches of 500 and 800 ppm windows were used in the exploratory ^{119}Sn and ^{195}Pt NMR analyses, respectively.

Chemicals. K_4Sn_9 was prepared by high-temperature fusion (1000 °C) of stoichiometric ratios of the elements. The chemicals were sealed in evacuated, silica tubes and carefully heated with a natural gas/oxygen flame. ***Caution:*** *molten alloy synthesis can result in serious explosion, and reactions should be conducted with great caution behind blast shields.* 4,7,13,16,21,24-Hexaoxa-1,10-diazobicyclo[8.8.8]hexacosane (2,2,2-crypt) was purchased from Aldrich, and $Pt(PPh_3)_4$ and Pt(TMTVS) where TMVTS = 2,4,6,8-tetramethyl-2,4,6,8-tetravinylcyclotetrasiloxane were purchased from Strem. Tris(bicyclo[2.2.1]heptene)-platinum(0) (i.e., $Pt(norbornene)_3$) was prepared according to literature

(47) Kunnen, B.; Niepmann, D.; Jeitschko, W. *J. Alloys Compd.* **2000**, *309*, 1−9.
(48) Verbeek, H.; Sachtler, W. M. H. *J. Catal.* **1976**, *42*, 257.
(49) Fearon, J.; Watson, G. W. *J. Mater. Chem.* **2006**, *16*, 1989−1996.
(50) Moses, M.; Fettinger, J. C.; Eichhorn, B. W. *Inorg. Chem.* **2007**, *46*, 1036−1038.
(51) Crascall, L. E.; Spencer, J. L. *Inorg. Synth.* **1990**, *28*, 126−129.
(52) Moses, M. J.; Fettinger, J. C.; Eichhorn, B. W. *Science* **2003**, *300*, 778−780.

methods.[51] Anhydrous ethylenediamine (en) and dimethylformamide (dmf) were purchased from Fisher, vacuum distilled from K_4Sn_9, and stored under dinitrogen. Toluene was distilled from sodium/benzophenone under dinitrogen and stored under dinitrogen.

Synthesis. Preparation of [K(2,2,2-crypt)]$_4$[Sn$_{17}$Pt$_2$]•en: Method 1. In vial 1, K_4Sn_9 (80 mg, 0.065mmol) was dissolved in en (ca. 2 mL) producing a red solution. In vial 2, $Pt(PPh_3)_4$ (80 mg, 0.065mmol) was dissolved in toluene (ca. 2 mL) producing a yellow solution. The contents of vial 2 were added to the contents of vial 1. 4 equiv of crypt (98 mg, 0.26mmol) were then added as a solid, and the reaction mixture was stirred for 30 min yielding a dark red-brown solution. The reaction mixture was filtered through tightly packed glass wool in a pipet and stored for 7 days. After removing the dark red crystals of $[K(2,2,2\text{-crypt})]_2[Pt@Sn_9Pt(PPh_3)]$, the solution was triturated with toluene and filtered through tightly packed glass wool in a pipet. Dark red crystals of the title complex formed in the reaction vessel after an additional 24 h. (10 mg, 12%) 25 °C δ (ppm) ^{119}Sn NMR (dmf): δ (ppm) −742 ($J_{^{195}Pt-^{119}Sn}$ = 774 Hz; $^1J_{^{119/117}Sn-^{119}Sn}$ = 170 Hz.). ^{195}Pt NMR (dmf): δ (ppm) −5700 ($J_{^{195}Pt-^{119}Sn} \approx$ 780 Hz).

Alternative Synthesis of [K(2,2,2-crypt)]$_4$[Sn$_{17}$Pt$_2$]: Method 2. In vial 1, K_4Sn_9 (80 mg, 0.065mmol) and 4 equiv of crypt (98 mg, 0.26mmol) were dissolved in en (ca. 2 mL) producing a red solution. In vial 2, 1 equiv of tris(bicyclo[2.2.1]heptene)platinum(0) (32 mg, 0.067mmol) was dissolved in toluene (ca. 0.5 mL) producing a yellow-brown solution. The contents of vial 2 were added to the contents of vial 1, and the reaction mixture was stirred overnight (ca. 22 h). The reaction mixture was then heated at 50 °C for 5 min, immediately filtered through tightly packed glass wool in a warm pipet, and stored. After 6 days, the solution was refiltered through tightly packed glass wool at room temperature and again after 10 more days. Dark red-brown crystals (12 mg, 13%) then formed in the reaction vessel. Platinum(0) 2,4,6,8-tetramethyl-2,4,6,8-tetravinylcyclotetrasiloxane complex solution (312 μL, 0.0325 mmol) can also be used to prepare the [K(2,2,2-crypt)]$_4$[Sn$_{17}$Pt$_2$] but does not yield crystalline solids. The product was characterized by ^{119}Sn NMR: δ (ppm) −742 ($J_{^{195}Pt-^{119}Sn}$ = 774 Hz; $^1J_{^{119/117}Sn-^{119}Sn}$ = 170 Hz.).

Preparation of [K(2,2,2-crypt)]$_3$[Pt@Sn$_9$H]. The [K(2,2,2-crypt)]$_3$[Pt@Sn$_9$H] is generated as a byproduct in method 1 above. The complex was formed 24 h after the reactants were mixed in an en/toluene solvent mixture as detected by ^{119}Sn NMR. 25 °C δ (ppm) ^{1}H NMR (en/tol): −22.3 ($J_{^1H-^{119/117}Sn}$ = 46 Hz; $J_{^{195}Pt-^1H}$ = 32 Hz). ^{119}Sn NMR (en/tol): δ (ppm) −369 ($J_{^{195}Pt-^{119}Sn}$ = 1540 Hz; $J_{^{119/117}Sn-^{119}Sn}$ = 160 Hz, $J_{^{1}H-^{119/117}Sn}$ = 46 Hz). ^{195}Pt NMR (dmf): δ (ppm) −5700 ($J_{^{195}Pt-^{119}Sn}$ = 1540 Hz, $J_{^{195}Pt-^1H}$ = 32 Hz).

Structural Studies: A dark-red prism of [K(2,2,2-crypt)]$_4$[Pt$_2$Sn$_{17}$]•3($C_2H_8N_2$), approximate dimensions 0.125 × 0.190 × 0.290 mm^3, was mounted in a drybox, transferred to the goniometer, and cooled to 220-(2) K. Data were collected on a Bruker Smart1000 X-ray diffraction system. A total of 3024 frames were collected to give a total of 40 278 reflections to a maximum 2θ angle of 27.50° in triclinic symmetry. Data were corrected for absorption effects with the semiempirical from equivalents method using SADABS; minimum and maximum transmission coefficients were 0.292 and 0.500.

The structure was solved and refined using the SHELXS-97 and SHELXL-97 software in the space group $P\bar{1}$ with Z = 1. The final anisotropic full-matrix least-squares refinement on F^2 with 911 variables converged at R_1 = 3.72% for the observed data and wR_2 = 8.79% for all data. The largest peak on the final difference map was 1.596 e$^-$/Å^3, and the largest hole was −1.519 e$^-$/Å.^{3} On the basis of the final model, the calculated density was 2.181 g/cm^3, and F(000), 2008 e$^-$.

Acknowledgment. This material is based upon work supported by the National Science Foundation under Grant No. 0401850. J. E. H. was supported under an HHMI Fellowship awarded to the University of Maryland.

Supporting Information Available: $Pt_2@Sn_{17}^{4-}$ crystal structure and additional drawings of the $Pt_2@Sn_{17}^{4-}$ ion. This material is available free of charge via the Internet at http://pubs.acs.org.

JA065764E